J. Fluid Mech. (1982), *vol.* 121, *pp.* 465–485
Printed in Great Britain

Nonlinear waves near a cut-off frequency in an acoustic duct – a numerical study

By J. A. ARANHA,† D. K. P. YUE‡ AND C. C. MEI

Department of Civil Engineering,
Massachusetts Institute of Technology,
Cambridge, Massachusetts 02139

(Received 19 September 1980 and in revised form 11 February 1982)

Cut-off frequencies are well known in acoustic ducts to be the thresholds of propagation and evanescence. If at one end of a duct the piston oscillates at very near the cut-off frequency, cross-duct resonance occurs and the linearized theory breaks down. This paper studies the nonlinear response, near a cut-off frequency of a guided wave, as an initial-boundary-value problem. The asymptotic state is shown to be governed by a modified cubic Schrödinger equation. Numerical solutions are then obtained for inputs of finite and long duration. In addition to the characteristics of the input envelope, two quantities control the transient phenomenon: frequency detuning and nonlinearity. Under certain circumstances, energy can be trapped near the piston long after a short-lived input has expired, while for a sustained input there is no sign of a steady state. Dissipation is not considered.

1. Introduction

Cut-off frequencies are commonly associated with unidirectional wave guides in various physical contexts. One of the most familiar guides with such a feature is an acoustic duct (see e.g. Morse & Ingard 1968). It is well known that there exists a discrete set of frequencies, each of which is a threshold of a new propagating mode. Below the threshold the mode changes drastically to an evanescent wave. According to the linearized theory, the response to a sinusoidally driven piston at one end becomes indefinitely large if the driving frequency approaches a cut-off frequency. The physical reason for such a growth is the vanishing of the relevant group velocity and the consequent entrapment of energy near the piston. Because a cut-off frequency is a natural frequency for the two-dimensional vibration in the cross-sectional plane, the breakdown is also referred to as the *cross-duct resonance* in the acoustics literature. Viscous effects and the elasticity of the piston or of the duct walls are two possible avenues by which the linearized theory can be rescued to yield finite responses.

In a semi-infinite water channel with a uniform rectangular cross-section, there exists also a set of cut-off frequencies for gravity wave modes which are non-uniform in the direction across the width of the channel. These modes can be produced by a piston performing sinusoidal rotational oscillations about a vertical axis. Again, excitation near a cut-off produces large responses (Ursell 1952). Mahony (1971)

† Now at Instituto de Pesquisas Technólogicas, Divisão de Engenharia Civil, São Paulo, Brazil.

‡ Now at Science Applications Inc., 1220 Prospect Street, La Jolla, CA 92038.

considered the effect of nonlinearity on the free surface, but only treated the steady state which is periodic with the same frequency as the piston. A nonlinear ordinary differential equation for the complex amplitude C was obtained,

$$C_{xx}+\lambda C+\nu|C|^2C=0, \tag{1.1}$$

where ν is a constant, and λ is the detuning factor, proportional to the difference between the actual frequency and the cut-off frequency ($\lambda > 0$ above cut-off, $\lambda < 0$ below cut-off). At the piston the boundary condition was $C(0) = 1$, but at infinity Mahony chose a special radiation condition such that $A \propto e^{ikx}$ for $\lambda > 0$ (above cut-off), and $C \propto e^{-kx}$ below cut-off, as in the linearized theory. On an amplitude–frequency diagram the final solution was not unlike that for a nonlinear spring. Ockendon & Ockendon (1973) also studied similar problems with essentially the same assumptions. They discussed certain non-uniqueness in the choice of the radiation condition and suggested that a stability consideration would be needed as in the case of a nonlinear spring. More recently Barnard, Mahony & Pritchard (1977) extended the theory of Mahony (1971) and performed laboratory experiments. A term accounting for the cumulative effect of viscous damping in the boundary layers was added to the governing equation. The damping coefficient was determined from an accompanying experiment for standing waves. The modified equation was integrated from a point in the far field towards the wavemaker so that the boundary condition on the wavemaker was met. Barnard *et al.* pointed out that the inviscid solution was non-unique, and suggested the study of an initial-value problem.

As cut-off frequencies are of general interest in waveguides, an examination of certain initial-value problems is interesting in its own right, in addition to shedding light on the theoretical question of whether a sinusoidal forcing necessarily leads to a steady periodic response at the driving frequency in the limit of large t. In this paper a physically simple case of a uniform fluid duct with rigid walls is treated. The approximate governing equation is found to be a cubic nonlinear Schrödinger equation which appears in many physical contexts:

$$iC_t+C_{xx}+\nu|C|^2C+\lambda C=0. \tag{1.2}$$

Numerical results are presented for inputs of both finite and very long durations, and contrasted with linear results. Evidence will be given to show that the transient response to a short-lived input envelope depends critically on the sign of detuning (above or below cut-off) and on the sign of nonlinearity. For a sustained input there are cases where a steady state is not reached.

2. An acoustic duct of uniform cross-section

Consider a uniform semi-infinite duct. At the end $x = 0$, a rigid piston oscillates at the frequency ω. The exact nonlinear equations for an isentropic flow can be reduced to the following (e.g. Keller & Millman 1971)

$$\phi_t+\tfrac{1}{2}(\nabla\phi)^2+\int_{p_0}^{p}\frac{dp}{\rho(p)}=0, \tag{2.1}$$

$$\frac{dp}{d\rho}\nabla^2\phi-\phi_{tt}=2\nabla\phi\,.\,\nabla\phi_t+\tfrac{1}{2}(\nabla\phi\,.\,\nabla)(\nabla\phi)^2, \tag{2.2}$$

where ∇ stands for the three-dimensional gradient operator, to be distinguished from the two-dimensional operator $\nabla^2 = \partial_y^2 + \partial_z^2$ used later. The following equation of state will be adopted:

$$p - p_0 = K[(\rho/\rho_0)^\gamma - 1], \tag{2.3}$$

where $K = p_0$, $\gamma = 1{\cdot}4$ for a perfect gas, and $K = \rho_0(\partial p/\partial\rho)_0$, $\gamma = 1$ for water. From (2.3) it may be deduced that

$$U^2 - U_0^2 = (\gamma - 1)\int_{p_0}^{p} \frac{dp}{\rho(p)}, \tag{2.4}$$

with $U^2 = dp/d\rho$, $U_0^2 = (dp/d\rho)_0$.

Equation (2.2) may be written for ϕ as follows:

$$U_0^2\nabla^2\phi - \frac{\partial^2\phi}{\partial t^2} = 2\nabla\phi\,.\,\nabla\frac{\partial\phi}{\partial t} + \tfrac{1}{2}(\nabla\phi\,.\,\nabla)(\nabla\phi)^2 + (\gamma-1)\left[\frac{\partial\phi}{\partial t} + \tfrac{1}{2}(\nabla\phi)^2\right]\nabla^2\phi. \tag{2.5}$$

Let us introduce the following dimensionless variables:

$$\left.\begin{aligned} \phi' &= \phi/U_0 a, \quad p' = p/K, \quad \rho' = \rho/\rho_0, \\ t' &= tU_0/a, \quad (x', y', z') = (x, y, z)/a, \end{aligned}\right\} \tag{2.6}$$

where a is the cross-sectional dimension of the duct. After dropping the primes the dimensionless form of (2.5) is obtained simply by replacing U_0 by unity. In dimensionless variables the boundary conditions are

$$\partial\phi/\partial n = 0 \quad \text{on } \partial S \text{ (duct walls)}, \tag{2.7}$$

$$\frac{\partial\phi}{\partial x} = \epsilon\left(\frac{\partial\xi}{\partial t} + \nabla\phi\,.\,\nabla\xi\right) \quad \text{on} \quad x = \epsilon\xi(y,z,t) = \epsilon\left[\frac{f}{-i\omega_n}e^{-i\Omega t} + *\right], \tag{2.8}$$

$$\phi \to 0 \quad \text{as} \quad x \sim +\infty \quad \text{for} \quad t < \infty, \tag{2.9}$$

$$\phi = \partial\phi/\partial t = 0 \quad (t = 0,\ 0 < x < \infty). \tag{2.10}$$

The small parameter ϵ is the measure of piston amplitude, and depends on x and y. The frequency ω_n is the eigenvalue associated with the orthonormal eigenfunction $h_n(y, z)$, both of which are defined by the following equations:

$$\nabla^2 h_n + \omega_n^2 h_n = 0 \quad \text{in } S \text{ (fluid in duct)}, \tag{2.11}$$

$$\partial h_n/\partial n = 0 \quad \text{on } \partial S, \tag{2.12}$$

where $\omega_0 < \omega_1 < \omega_2 < \ldots$. Note that $\omega_0 = 0$ and $h_0 = 1$. Clearly h_n is a natural mode in the cross-sectional plane.

The *linearized* steady-state response to an input of frequency Ω can be expressed as

$$\phi = \epsilon\sum_{m=0}^{\infty} h_m(y,z)\,(C_m(x)\,e^{-i\Omega t} + *), \tag{2.13a}$$

where

$$\left.\begin{aligned} C_m &= -\frac{if_m}{(\Omega^2 - \omega_m^2)^{\frac{1}{2}}}\exp[i(\Omega^2 - \omega_m^2)^{\frac{1}{2}}x] \quad (\Omega > \omega_m) \\ &= \frac{f_m}{(\omega_m^2 - \Omega^2)^{\frac{1}{2}}}\exp[-(\omega_m^2 - \Omega^2)^{\frac{1}{2}}x] \quad (\Omega < \omega_m), \end{aligned}\right\} \tag{2.13b}$$

with

$$f_m \equiv \langle f, h_m\rangle \equiv \int\int_S f h_m\,dy\,dz \tag{2.13c}$$

being the inner product integrated over the cross-section, and f independent of t. If, however, Ω is close to a particular ω_m and $f_m \neq 0$, then this solution is no longer as small as $O(\epsilon)$, and the linearized approximation fails. Moreover, the variation of C_m can be rewritten as

$$e^{-i\omega_m t}\exp\left[i(\Omega^2-\omega_m^2)^{\frac{1}{2}}x - i(\Omega^2-\omega_m^2)\,t/2\omega_m\right] \quad (\Omega > \omega_m) \tag{2.14a}$$

or

$$e^{-i\omega_m t}\exp\left[-(\omega_m^2-\Omega^2)^{\frac{1}{2}}x - i(\Omega^2-\omega_m^2)\,t/2\omega_m\right] \quad (\Omega < \omega_m), \tag{2.14b}$$

which shows a slow modulation in x and t. Now let α be formally defined by

$$\left.\begin{aligned}\Omega &= \omega_m + (\lambda/2\omega_m)\,\epsilon^{2(1-\alpha)},\\ \Omega^2-\omega_m^2 &= O(\epsilon^{2(1-\alpha)}),\end{aligned}\right\} \tag{2.15}$$

or equivalently,

with $\lambda = O(1)$ being the detuning parameter. We must then anticipate the need for the slow variables $X = x\epsilon^{1-\alpha}$ and $T = t\epsilon^{2(1-\alpha)}$, with α still unknown.

For simplicity we shall assume $\omega_m' = O(1)$ (i.e. low modes) so that the order-of-magnitude assumption behind (2.15) need not be modified.

We now focus attention on a neighbourhood of the cut-off frequency ω_n. For simplicity

$$f \equiv f_n h_n(y,z) \tag{2.16}$$

is assumed, leaving the more general case for later comment. It may be seen from (2.5) that at $O(\epsilon^{2\alpha})$ the quadratic forcing terms contain only second harmonics. Assuming that $2\omega_n$ is not a resonant frequency, there is no secularity at $O(\epsilon^{2\alpha})$. At $O(\epsilon^{3\alpha})$ the cubic terms lead to secular first harmonics which must be removed by adding $\epsilon^{2-\alpha}(\partial^2\phi_1/\partial t\,\partial T, \partial^2\phi_1/\partial X^2)$; therefore $\alpha = \frac{1}{2}$, as in Mahony (1971). We now introduce

$$X = \epsilon^{\frac{1}{2}}x, \quad T = \epsilon t/2\omega_n, \quad \Omega = \omega_n + \lambda\epsilon/2\omega_n, \tag{2.17}$$

and the perturbation expansion

$$\phi = \epsilon^{\frac{1}{2}}\phi_1 + \epsilon\phi_2 + \epsilon^{\frac{3}{2}}\phi_3 + \ldots, \quad \phi_j = \phi_j(x,y,z,t,X,T). \tag{2.18}$$

The implied perturbation equations from (2.5) can be obtained in a routine manner. We note first that the boundary condition on the piston becomes

$$\left(\frac{\partial}{\partial x} + \epsilon^{\frac{1}{2}}\frac{\partial}{\partial X}\right)(\epsilon^{\frac{1}{2}}\phi_1 + \epsilon\phi_2 + \ldots) + \epsilon^{\frac{3}{2}}h_n\frac{\partial^2\phi_1}{\partial x^2}\left(\frac{f}{-i\omega_n}e^{-i\omega t} + *\right) + O(\epsilon^{\frac{5}{2}})$$
$$= \epsilon(f e^{-i\Omega t} + *) + \epsilon^{\frac{3}{2}}\nabla\phi_1 \cdot \left[\frac{\nabla f}{-i\omega_n}e^{-i\Omega t} + *\right] + \ldots \tag{2.19}$$

on $x = 0$. The governing equations for ϕ_1 are

$$\nabla^2\phi_1 - \frac{\partial^2\phi_1}{\partial t^2} = 0 \quad \text{in } S, \tag{2.20a}$$

$$\frac{\partial\phi_1}{\partial n} = 0 \quad \text{on } \partial S, \tag{2.20b}$$

$$\frac{\partial\phi_1}{\partial X} = f e^{-i\Omega t} + * \quad \text{at} \quad X = 0, \tag{2.20c}$$

$$\frac{\partial\phi_1}{\partial x} = 0 \quad \text{at} \quad x = 0. \tag{2.20d}$$

The solution can be easily shown to be independent of the fast co-ordinate x, hence $\mathbf{\nabla}$ reduces to ∇, and

$$\phi_1 = \phi_{10}(X,T) + h_n(y,z)\,[C(X,T)\,e^{-i\Omega t} + *], \tag{2.21}$$

subject to

$$\partial\phi_{10}/\partial X = 0, \quad \partial C/\partial X = f \quad \text{on} \quad X = 0 \tag{2.22a, b}$$

in view of (2.20c).

At $O(\epsilon)$ the governing equations are

$$\mathbf{\nabla}^2\phi_2 - \frac{\partial^2\phi_2}{\partial t^2} = q_{22}(iCe^{-2i\Omega t} + *) \quad \text{in } S, \tag{2.23a}$$

$$\partial\phi_2/\partial n = 0 \quad \text{on } \partial S, \tag{2.23b}$$

$$\partial\phi_2/\partial x = 0 \quad \text{at} \quad x = 0, \tag{2.23c}$$

where

$$q_{22} = -2\omega_n(\nabla h_n)^2 + (\gamma-1)\,\omega_n^2 h_n^2. \tag{2.23d}$$

The solution is again independent of x, and may be given explicitly by

$$\phi_2(y,z,t,X,T) = \Psi_2(iCe^{-2i\Omega t} + *), \tag{2.24a}$$

with

$$\psi_2(y,z) = \sum_{m=0}^{\infty} (4\omega_n^2 - \omega_m^2)^{-1} \langle q_{22}, h_m\rangle h_m, \tag{2.24b}$$

where $\langle a,b\rangle$ denotes a scalar product defined as in (2.13c). Note that, from (2.22b) and (2.24a),

$$\left.\frac{\partial\phi_2}{\partial X}\right|_{X=0} = \psi_2(ife^{-2i\Omega t} + *). \tag{2.25}$$

At $O(\epsilon^{\frac{3}{2}})$ we have

$$\mathbf{\nabla}^2\phi_3 - \frac{\partial^2\phi_3}{\partial T^2} = q_{31}(|C|^2 Ce^{-i\Omega t} + *) - h_n\left[\left(\frac{\partial^2 C}{\partial X^2} + i\frac{\partial C}{\partial T} + \lambda C\right)e^{-i\Omega t} + *\right] + q_{33}(C^3 e^{-3i\Omega t} + *) - \frac{\partial^2\phi_{10}}{\partial X^2}, \tag{2.26a}$$

$$\partial\phi_3/\partial n = 0 \quad \text{on } \partial S, \tag{2.26b}$$

$$\frac{\partial\phi_3}{\partial x} = [(\nabla h_n)^2\omega_n - 2\psi_2]\,(if_n Ce^{-2i\Omega t} + *) + (\nabla h_n)^2\left(\frac{Cf_n^*}{i\omega_n} + *\right) \quad \text{on} \quad x = 0, \tag{2.26c}$$

where

$$q_{31} = 2(\nabla h_n \,.\, \nabla\psi_2)\,\omega_n + (\gamma-1)\,[-\omega_n h_n \nabla^2\psi_2 + 2\omega_n\psi_2\nabla^2 h_n] + \tfrac{3}{2}(\nabla h_n \,.\, \nabla)\,(\nabla h_n)^2 + \tfrac{3}{2}(\gamma-1)\,(\nabla h_n)^2\nabla^2 h_n, \tag{2.26d}$$

$$q_{33} = 2(\nabla h_n \,.\, \nabla\psi_2)\,3\omega_n + (\gamma-1)\,(\omega_n h_n\nabla^2\psi_2 + 2\omega_n\psi_2\nabla^2 h_n) + \tfrac{1}{2}(\nabla h_n \,.\, \nabla)\,(\nabla h_n)^2 + \tfrac{1}{2}(\gamma-1)\,(\nabla h_n)^2\nabla^2 h_n. \tag{2.26e}$$

Notice that both q_{31} and q_{33} are functions of y and z only. The solution ϕ_3 may be divided into two parts, one of which is independent of x and accounts for the forcing terms in (2.26a), while the other depends on x and accounts for (2.26c):

$$\phi_3 = \phi_3^{(1)}(y,z,t,X,T) + \phi_3^{(2)}(x,y,z,t). \tag{2.27}$$

Referring to (2.21), since $h_n(Ce^{-i\Omega T} + *)$ is the homogeneous solution to the two-

dimensional (y, z) problem governing ϕ_3, the first harmonic terms on the right-hand side of (2.26a) must be orthogonal to h_n (Fredholm alternative). Thus

$$i\frac{\partial C}{\partial T}+\lambda C+\frac{\partial^2 C}{\partial X^2}+K|C|^2C=0, \tag{2.28a}$$

where

$$K=-\langle q_{31}, h_n\rangle. \tag{2.28b}$$

In addition, C must satisfy (2.22b), and vanishes both at $X\to+\infty$ for all t and $T=0$ for all X.

Finally, solvability for the zeroth harmonic ϕ_{30} requires that

$$\partial^2\phi_{10}/\partial X^2=0 \quad (X>0). \tag{2.29}$$

It follows from (2.22a) that $\partial\phi_{10}/\partial X=0$ for all $X>0$. Thus ϕ_{10} depends only on T and possibly on x in a much slower manner; its effect on the dynamic pressure is at most of the order of $\epsilon^{\frac{3}{2}}\partial\phi_{10}/\partial T$. Limiting our attention to the leading order $O(\epsilon^{\frac{1}{2}})$, it is only necessary to solve for C.

Equation (2.28a) with $\lambda=0$ appears in nonlinear optics and in water waves; in both cases the sign of K is known to affect the physics in important ways. In optics (Karpman 1975), $K>0$ corresponds to self-focusing, and $K<0$ to defocusing; while in water waves $K>0$ corresponds to instability, and $K<0$ to stability to side-band disturbances. It is thus important to know first the sign of K for an acoustic duct. Since (2.28b) is unfortunately too complicated for any general conclusion, we examine the special case of a circular duct with axially symmetric cut-off modes. The nth normalized eigenfunction is

$$h_n=J_0(\omega_n r)/\pi^{-\frac{1}{2}}J_0(\omega_n),$$

where $\omega_1=3{\cdot}8317$, $\omega_2=7{\cdot}0156$, $\omega_3=10{\cdot}1735\ldots$ are the roots of $J_0'(\omega_n)=0$. By computing the scalar products of (2.24b) and (2.28b) numerically we obtain the following values for the first few modes:

$$\begin{aligned}&\text{for air} \quad (\gamma=1{\cdot}4) \quad K=-1{\cdot}096,\ -2{\cdot}798,\ -18{\cdot}305,\ldots;\\ &\text{for water} \quad (\gamma=1{\cdot}0) \quad K=27{\cdot}31,\ldots.\end{aligned}$$

The large numerical values of K are due to the facts that $K=O(\omega_n^3)$ and that ω_1 is already close to 4. It is therefore convenient to renormalize the variables as follows:

$$\left.\begin{aligned}\hat{T}&=[\tfrac{1}{2}|K|\bar{f}_n^2]^{\frac{1}{2}}T, \quad \hat{X}=[\tfrac{1}{2}|K|\bar{f}_n^2]^{\frac{1}{2}}X,\\ \hat{\lambda}&=\left[\frac{2}{|K|\bar{f}_n^2}\right]^{\frac{1}{2}}\lambda, \quad \hat{A}(\hat{X},\hat{T})=\frac{2}{\bar{f}_n}(\tfrac{1}{2}|K|f_n^2)^{\frac{1}{2}}A(X,T),\end{aligned}\right\} \tag{2.30}$$

where $\bar{f}_n$ is the maximum of f_n. Modifications may be needed for very high modes, but are not pursued here.

The initial-boundary-value problem becomes

$$i\frac{\partial\hat{C}}{\partial\hat{T}}+\frac{\partial^2\hat{C}}{\partial\hat{X}^2}+\hat{\lambda}\hat{C}+2(\operatorname{sgn}K)\,|\hat{C}|^2C=0 \quad (\hat{X}>0,\ \hat{T}>0), \tag{2.31a}$$

$$\partial\hat{C}/\partial\hat{X}=\hat{f}_n(\hat{T}) \quad (\hat{X}=0,\ \hat{T}<\infty), \tag{2.31b}$$

$$\hat{C}\to 0 \quad (\hat{X}\to\infty,\ \hat{T}<\infty), \tag{2.31c}$$

$$\hat{C} = 0 \quad (\hat{X} > 0,\ \hat{T} = 0). \tag{2.31d}$$

From here on, we shall omit the symbol $\wedge$ for brevity.

Comments on degenerate cases. Of all elementary cross sections, the circular duct of radius a admits axially symmetric cross-duct modes

$$h_{0m}(r,\theta) \sim J_0(\omega_{0m} r) \quad \text{with} \quad J_0'(\omega_{0m}) = 0, \tag{2.32}$$

which can be dealt with by (2.28) without modification. However two different non-axially-symmetric modes can share the same cut-off frequency (degeneracy)†

$$\begin{bmatrix} h_{nm}^{(1)} \\ h_{nm}^{(2)} \end{bmatrix} \sim J_n(\omega_{nm} r) \begin{bmatrix} \cos m\theta \\ \sin m\theta \end{bmatrix}, \quad J_n'(\omega_{nm}) = 0 \quad (n = 1,2,3,\ldots;\ m = 1,2,3,\ldots). \tag{2.33}$$

For the doubly degenerate case we must assume at the leading order

$$\phi_1 = \phi_{10} + \{[C_1(X,T)\, h_n^{(1)}(y,z) + C_2(X,T)\, h_n^{(2)}(y,z)]\, e^{-i\Omega t} + *\}. \tag{2.34}$$

It can then be shown that C_1 and C_2 are governed by coupled simultaneous equations of the following type:

$$i\frac{\partial C_n}{\partial T} + \lambda C_n + \frac{\partial^2 C_n}{\partial X^2} + \{|C_1|^2(K_{n1}C_1 + K_{n2}C_2) + |C_2|^2(K_{n3}C_1 + K_{n4}C_2) + K_{n5}C_1^* C_2^2 + K_{n6}C_2^* C_1^2\} = 0 \quad (n = 1,2), \tag{2.35}$$

subject to the boundary condition

$$\partial C_n/\partial X = f_n \quad (X = 0, \quad T > 0), \tag{2.36}$$

and the C_n vanish as $X \to \infty$. These equations can be used to study the nonlinear energy transfer between two modes.

The case of a rectangular duct is infinitely degenerate. In normalized form the duct has dimensionless sides 2 and $2b$; the cross-duct (cut-off) frequencies are

$$\omega_{nm} = \tfrac{1}{4}(n^2 + m^2/b^2)^{\frac{1}{2}}.$$

Clearly $N\omega_{nm} = \omega_{Nn,Nm}$ for $N = 1,2,3,\ldots$. In principle, (2.34) must be generalized to an infinite series, and an infinite set of coupled equations resembling (2.35) will result.

Referring to (2.28), if K vanishes identically one must pursue terms up to the fourth order. It can then be shown that the slow variables must be $X = \epsilon^{\frac{3}{4}}x$ and $T = \epsilon^{\frac{3}{4}}t/2\omega_m$ and the cubic nonlinear term in (2.28) must be replaced by one of fourth order.

Lastly, if $f(y,z)$ contains other non-resonating components f_m $(m \neq n)$ in addition to f_n, it can also be shown that the regular part of the solution is $O(\epsilon)$ and does not affect the behaviour of C.

Details of all these modifications may be found in Aranha (1978).

† For a semicircular duct with a plane wall along the diameter $0 = 0, \pi$, only $\cos m\theta$ is relevant, and there is no degeneracy.

3. The linearized solution†

To provide a basis for comparison, it is instructive to examine the linearized solution to (2.31) first. For a constant envelope, $f_n(T) = H(T)$ in (2.31b), where H is the Heaviside function; the linearized solution can be obtained via Laplace transforms as

$$C(X,T) = -\frac{1+i}{(2\pi)^{\frac{1}{2}}}\int_0^T d\tau\,\frac{\exp\left[iX^2/4(T-\tau)+i\lambda(T-\tau)\right]}{(T-\tau)^{\frac{1}{2}}}. \tag{3.1}$$

The solution $C(X,T)$ for a rectangular envelope pulse of duration T_0 is simply

$$C(X,T) = \left.\begin{array}{ll} C(X,T) & (0 < T < T_0), \\ C(X,T) - C(X,T-T_0) & (T > T_0). \end{array}\right\} \tag{3.2}$$

For any time T, (3.1) or (3.2) can be integrated numerically for the spatial variation.

The time variation $C(0,T)$ of C at the piston can be obtained more explicitly. Setting $X = 0$ in (3.1), a change of variable gives

$$C(0,T) = \begin{cases} -(1+i)\,(2T/\pi)^{\frac{1}{2}} \quad (\lambda = 0), & (3.3a) \\ \left(\dfrac{i}{-1}\right)\dfrac{1}{|\lambda|^{\frac{1}{2}}}\operatorname{erf}\left[(\mp 1+i)\,(\tfrac{1}{2}|\lambda|T)^{\frac{1}{2}}\right] \quad (\lambda \lessgtr 0). & (3.3b) \end{cases}$$

For the critical case $\lambda = 0$ (at cut-off), $C(0,T)$ grows as $\sqrt{T}$ until the pulse expires. If the duration of the pulse is T_0, the total energy input by the piston is

$$E(T_0) = -2\mathscr{I}\int_0^{T_0} d\tau\, CC_x^*|_{x=0} = \frac{4}{3}\left(\frac{2}{\pi}\right)^{\frac{1}{2}} T_0^{\frac{3}{2}}. \tag{3.4}$$

After the expiration of the pulse, the piston pressure is

$$C(0,T) = -(1+i)\left(\frac{2}{\pi}\right)^{\frac{1}{2}}\frac{T_0}{T^{\frac{1}{2}}(1+(1-T_0/T)^{\frac{1}{2}})}, \tag{3.5}$$

which decreases as $T^{-\frac{1}{2}}$ for large T.

Away from cut-off, (3.3b), for $\lambda \neq 0$, can be written alternatively in terms of Fresnel integrals $\mathscr{C}$ and $\mathscr{S}$ as

$$C(0,T) = -\frac{1\pm i}{|\lambda|^{\frac{1}{2}}}\begin{bmatrix} \mathscr{C}\left(\left(\dfrac{2|\lambda|T}{\pi}\right)^{\frac{1}{2}}\right) + i\mathscr{S}\left(\left(\dfrac{2|\lambda|T}{\pi}\right)^{\frac{1}{2}}\right) \\ \mathscr{S}\left(\left(\dfrac{2|\lambda|T}{\pi}\right)^{\frac{1}{2}}\right) + i\mathscr{C}\left(\left(\dfrac{2|\lambda|T}{\pi}\right)^{\frac{1}{2}}\right) \end{bmatrix} \quad (\lambda \gtrless 0), \tag{3.6}$$

which oscillate and approach constant limits as $|\lambda|T \to \infty$:

$$C(0,T) \to -\binom{i}{1}|\lambda|^{-\frac{1}{2}}, \quad |\lambda|T \to \infty \quad (\lambda \gtrless 0). \tag{3.7}$$

This result can be taken as the steady-state limit for finite λ, or the limit of large $|\lambda|$ if T is kept fixed. If the input is of finite duration T_0, the time history for $t > T_0$ can be inferred from (32) and (3.6), and also diminishes as $T^{-\frac{1}{2}}$ for $T \gg 1$. For a sustained input and for $T_0 = 3$, figure 1 shows the following magnitude:

$$|C(0,T)| = \left\{\frac{2}{|\lambda|}\left[\mathscr{C}^2\left(\left(\frac{2|\lambda|T}{\pi}\right)^{\frac{1}{2}}\right) + \mathscr{S}^2\left(\left(\frac{2|\lambda|T}{\pi}\right)^{\frac{1}{2}}\right)\right]\right\}^{\frac{1}{2}}. \tag{3.8}$$

† An 'exact' linearized solution can also be constructed without the asymptotic approximation leading to (2.31a).

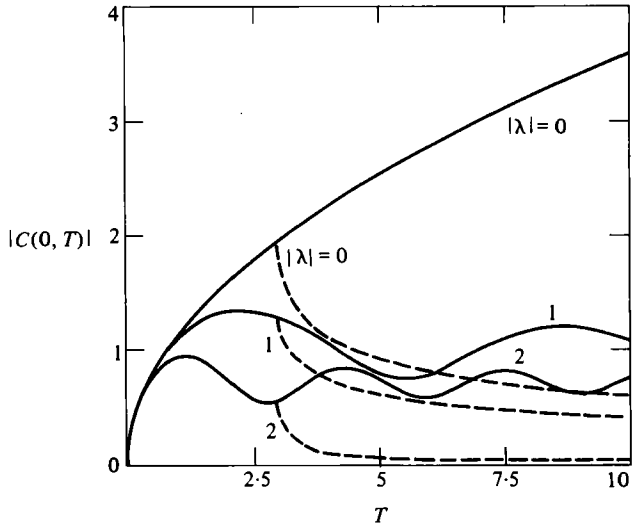

FIGURE 1. $|C(0,T)|$ for a sustained input (——) and a pulse input of duration $T_0 = 3$ (– – –) for the linearized problem.

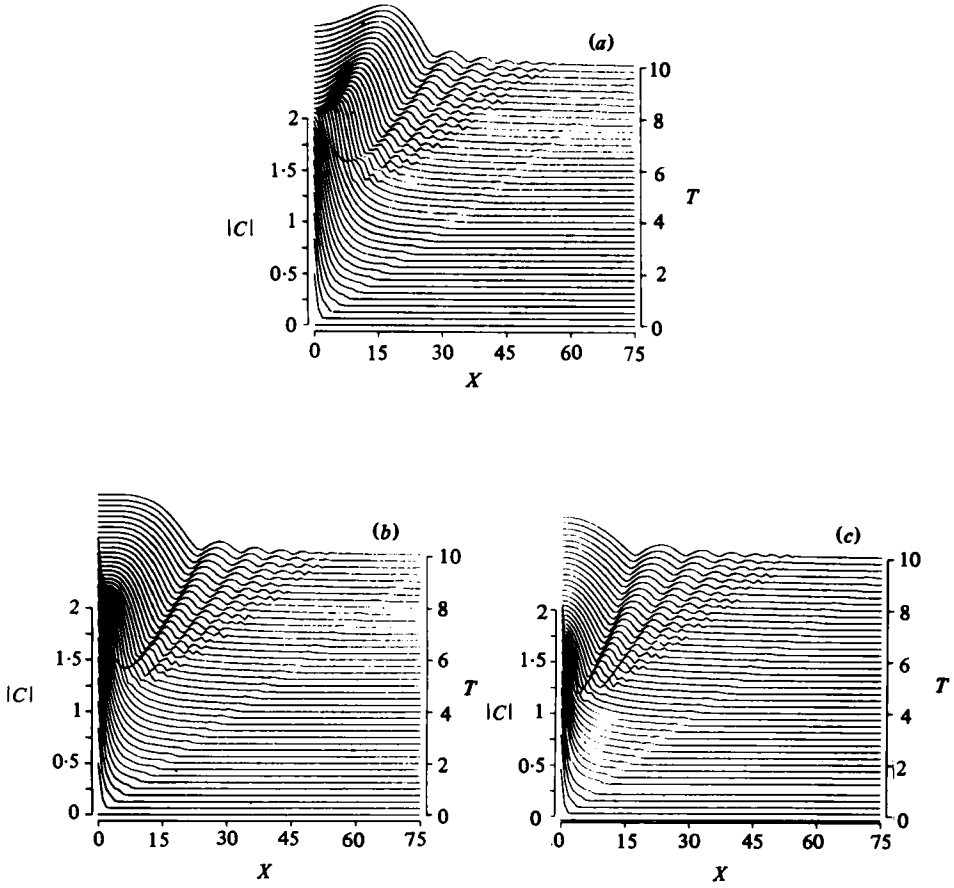

FIGURE 2. Evolution profiles $|C(X,T)|$ for the linearized problem.
(*a*) $\lambda = 1$; (*b*) 0; (*c*) -1.

Note that it does not depend on the sign of λ. The work done by the piston up to any time $T \leqslant T_0$ is

$$\left.\begin{aligned} E(T) &= -2\mathscr{I}\int_0^T d\tau\, CC_X^*\Big|_{X=0} \\ &= \frac{2}{|\lambda|^{\frac{1}{2}}}\int_0^T d\tau\left[\mathscr{C}\left(\left(\frac{2|\lambda|\tau}{\pi}\right)^{\frac{1}{2}}\right) \pm \mathscr{S}\left(\left(\frac{2|\lambda|\tau}{\pi}\right)^{\frac{1}{2}}\right)\right] \quad (\lambda \gtrless 0). \end{aligned}\right\} \tag{3.9}$$

From the known properties of Fresnel integrals, it can be shown that E increases monotonically with the pulse duration if $\lambda > 0$. For $\lambda < 0$, however, E oscillates with respect to the duration, so that a longer pulse does not necessarily imply greater energy input as one might suspect naively. Thus the sign change of λ changes the behaviour of the solution near the piston. The typical evolution profiles of $|C(X,T)|$ are shown in figures 2(*a–c*) for $T_0 = 3$ and $\lambda = 0, \pm 1$.

4. Numerical scheme for the nonlinar initial-boundary-value problem

Equations (2.31*a–d*) were solved numerically by a semi-implicit finite-difference scheme of the Crank–Nicolson type:

$$C^{n+1} = C^n + \tfrac{1}{2}i\Delta T(C_{XX}^{n+1} + \lambda C^{n+1} + 2(\operatorname{sgn} K)\,|\tilde{C}|^2 C^{n+1} + C_{XX}^n + \lambda C^n + 2(\operatorname{sgn} K)\,|C^n|^2 C^n), \tag{4.1}$$

where $C^n = C(n\Delta T)$, and the nonlinear term was quasi-linearized by the estimate

$$\tilde{C} = C^n + i\Delta T(C_{XX}^n + \lambda C^n + 2(\operatorname{sgn} K|C^n|^2 C^n). \tag{4.2}$$

Equation (4.2) has a truncation error $O(\Delta T)^2$, so that (4.1) has only $O(\Delta T)^3$ error at each step, or a global truncation error $O(\Delta T)^2$ for $T = O(1)$. The spatial derivatives were replaced by second-order centred differences, and a sufficiently large domain for X was decided by numerical experiments, so that up to a certain prescribed time the effects of the outer boundary were negligible. All the computations were checked to within a few per cent for the global energy conservation

$$E(T) \equiv -2\mathscr{I}\int_0^T dT'\,(CC_X^*)\Big|_{X=0} = \int_0^\infty dX'|C(X',T)|^2, \tag{4.3}$$

which can be deduced from (2.31*a*). Our experience shows that (4.1) is stable, and satisfactory results can be obtained without iteration for the nonlinear term if ΔT is sufficiently small.

As the basis for deciding the step sizes, the numerical scheme was tested against the known soliton solution of (2.31*a*). For $K > 0$, there exists a permanent wave of the form

$$C^s(X,T) = \pm a\operatorname{sech} a(X - X_0 - UT)\exp\{i[\tfrac{1}{2}U(X - X_0) - (\tfrac{1}{4}U^2a^2 - \lambda)\,T]\}, \tag{4.4}$$

where a, U are unrelated constants. In our numerical experiments, we chose X_0 sufficiently large and negative so that $C(X,0) = 0$ initially for all $X > 0$, and imposed the piston condition (2.31*b*) as

$$C_X(0,T) = C_X^s(0,T).$$

Our computed results were found to deviate by less than 2 or 3 % from (4.4) after the soliton had propagated a distance $O(10)$ times its width. The step sizes in all compu-

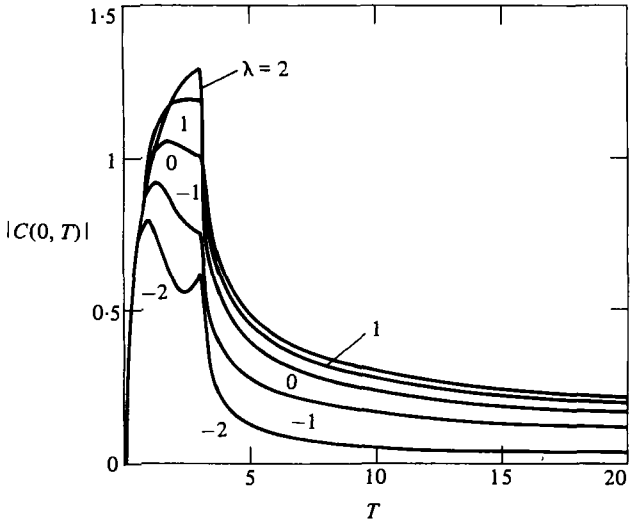

FIGURE 3. $|C(0,T)|$ for $T_0 = 2$, $K < 0$.

tations were $\Delta X = 0{\cdot}2$ and $\Delta T = 0{\cdot}025$. The total spatial extent was between five to seven times that corresponding to the total duration of computation.

Two types of piston condition were studied for $K \gtrless 0$. First we consider rectangular pulse inputs for $f_n(T)$, of unit amplitude and finite duration T_0, to give some understanding of the solutions of (2.31) for different sgn K, λ and T_0. Then, to see whether a steady-state solution can be ultimately reached, the initial-boundary-value problem was solved for steady forcing ($T_0 \to \infty$). In all our computations, it was found desirable to smooth the step jump of the input over a few time steps, which removed small high-frequency oscillations in the solution. The overall solution is only negligibly affected by such changes in the starting profile. Smooth transitions consisting of a half-sinusoid of duration $T_0 = O(1)$ at both ends of the pulse were also tested. These results involved an additional time scale, but were found not to differ qualitatively from those with step inputs; hence they are not discussed here.

5. Nonlinear response to envelope pulses of finite duration

5.1. *The case* $K < 0$

For an input of duration $T_0 = 3$, $|C(0,T)|$ is plotted in figure 3 for a range of λ. For $T < T_0$, the curves are qualitatively different from the linear predictions, especially for $\lambda \geqslant 0$. The amplitude attained was larger for greater λ. After the input pulse expired, the pressure on the piston decreased smoothly with time, which is similar to the linearized results. The spatial evolution for $|C|$ was quite similar for the different λs, and qualitatively similar to the linear results shown in figure 2. The disturbance moved away from the piston like a step front, with a spreading oscillatory front followed by a rather smooth and flat region, which decayed in height as time increased (cf. figure 3). Other values of T_0 were also computed with generally similar results, and are not presented.

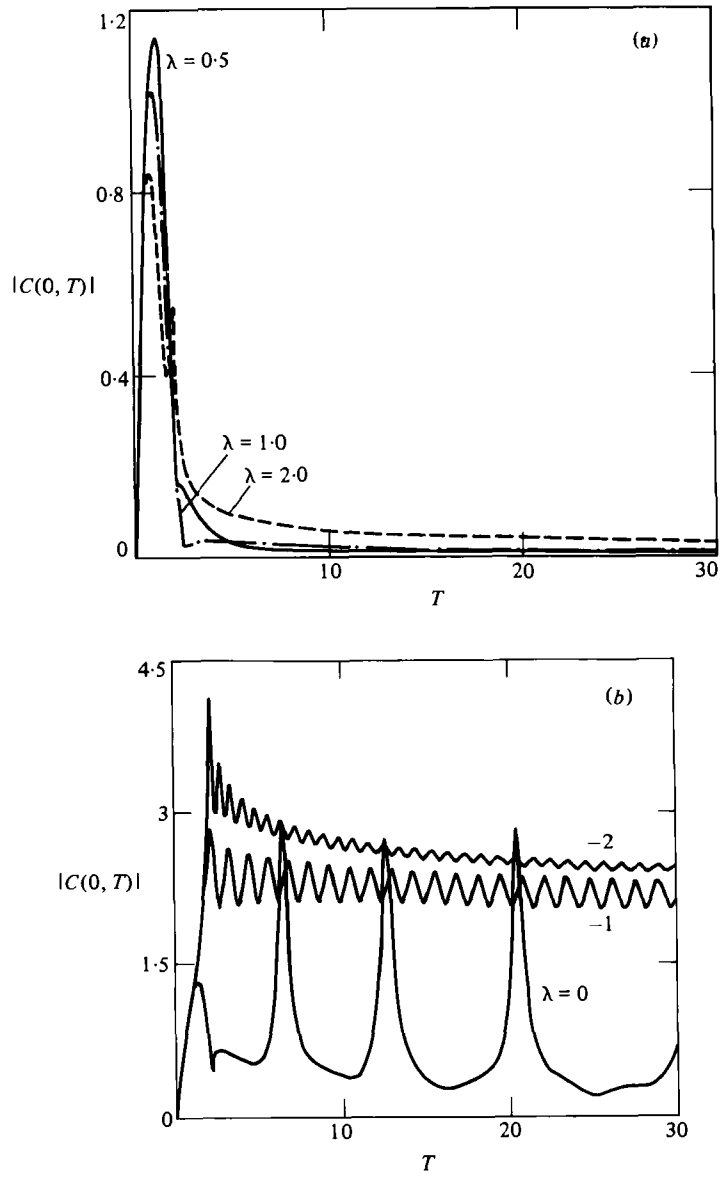

FIGURE 4. $|C(0, T)|$ for $T_0 = 2$, $K > 0$.

5.2. *The case* $K > 0$

This case exhibits the most interesting variety of features which are vastly different from the linearized results.

For a very short input of $T_0 = \frac{1}{2}$, the solution did not deviate very much from the linearized case. In particular, $|C(0, T)|$ grew as the input continued, but decayed in time after the pulse expired. The spatial variations resembled closely those of figure 2, and are omitted.

As the pulse length increases, deviations from the linear results became apparent. Figures 4(*a*, *b*) show $|C(0, T)|$ for $T_0 = 2$. The most striking difference is for $\lambda \leqslant 0$

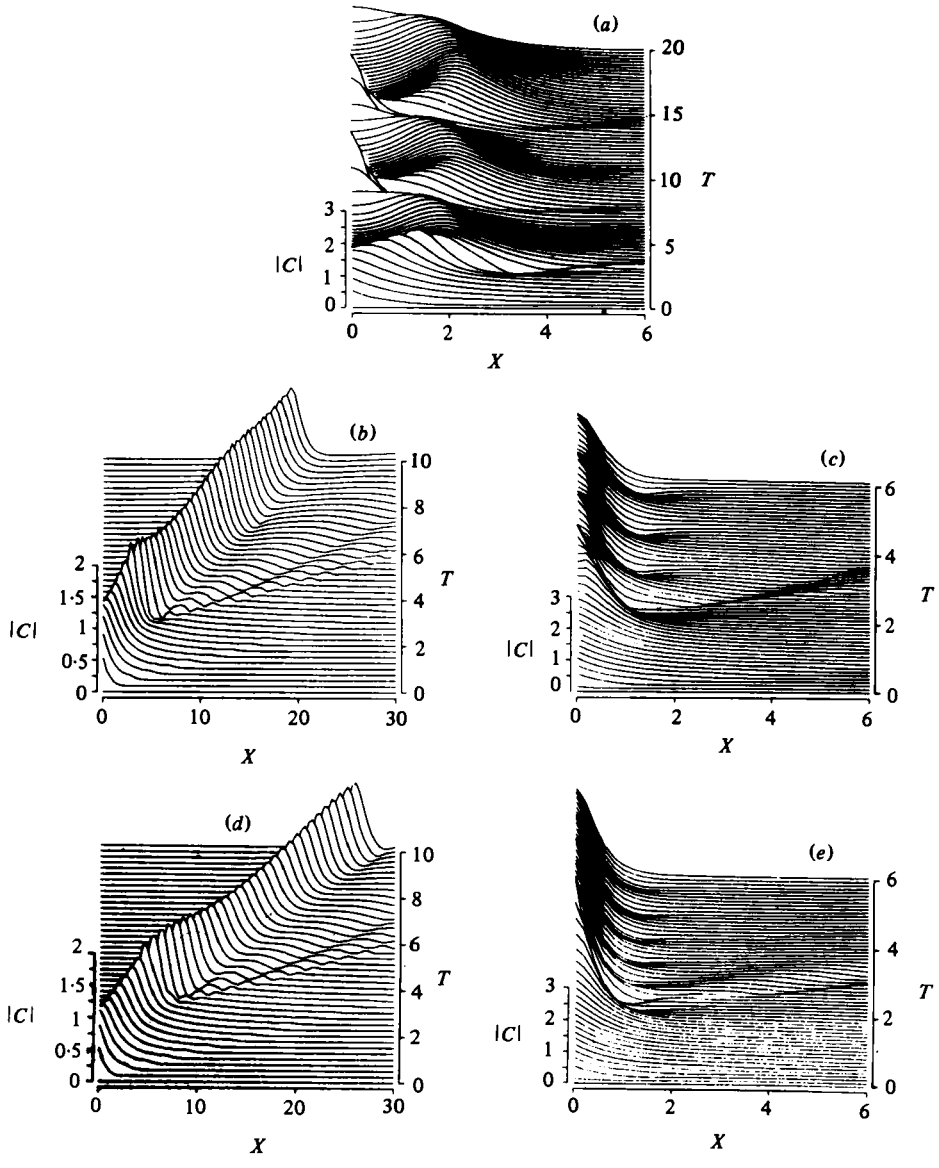

FIGURE 5. Space–time evolutions of $|C(X,T)|$; $T_0 = 2$, $K > 0$. Note that different scales are used to bring out the main features. (*a*) $\lambda = 0$; (*b*) 1; (*c*) -1; (*d*) 2; (*e*) -2.

(figure 4*b*), where $|C(0,T)|$ does not decay rapidly, but oscillates in time long after the input has ended at $T_0 = 2$. The space–time evolution is shown in figure 5. For $\lambda > 0$ (above cut-off), most of the energy was radiated away in a single leading peak, which propagated at a constant velocity with very little change in form. For $\lambda = 0$, -1, -2, there was some initial leak of energy into the undisturbed region, but most of the energy remained near the piston and underwent a periodic recurrence with little change in amplitude, in agreement with figure 4 (*b*). Thus energy trapping was manifest in an even stronger way in the nonlinear theory.

We have studied pulse inputs of even longer durations, $T_0 = 3$ and 5. Only the case

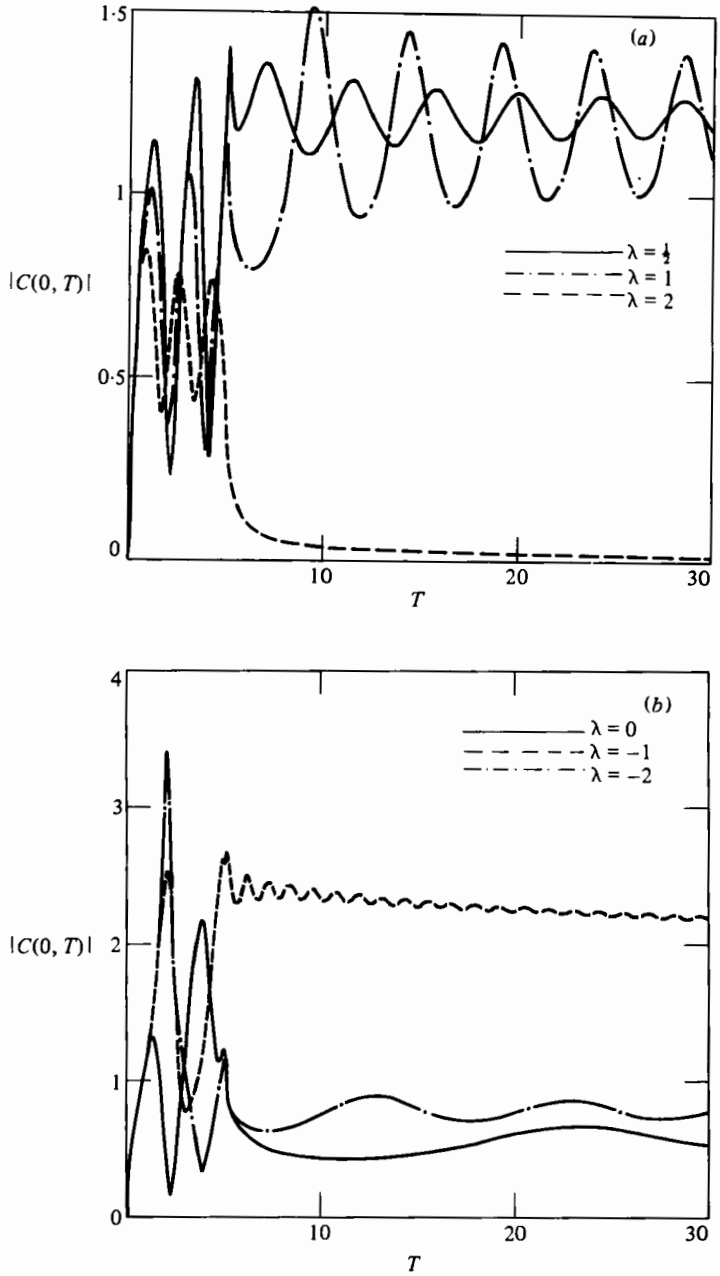

FIGURE 6. $|C(0, T)|$ for $T_0 = 5$, $K > 0$. (a) $\lambda > 0$; (b) $\lambda \leqslant 0$.

of $T_0 = 5$ is shown in figures 6(*a*, *b*) and 7. The main features are basically the same, i.e. above *some* threshold value of λ (close to but not necessarily zero) isolated peaks were radiated away. The number of such peaks increased with T_0 (one for $T_0 = 1, 2$, two for $T_0 = 3$ and three for $T_0 = 5$). Below the threshold, the dominant feature is that of trapping near $X = 0$, clearly shown in figure 6(*b*). Near the threshold value of λ, both peak radiation and trapping coexisted. By comparing graphs for various T_0,

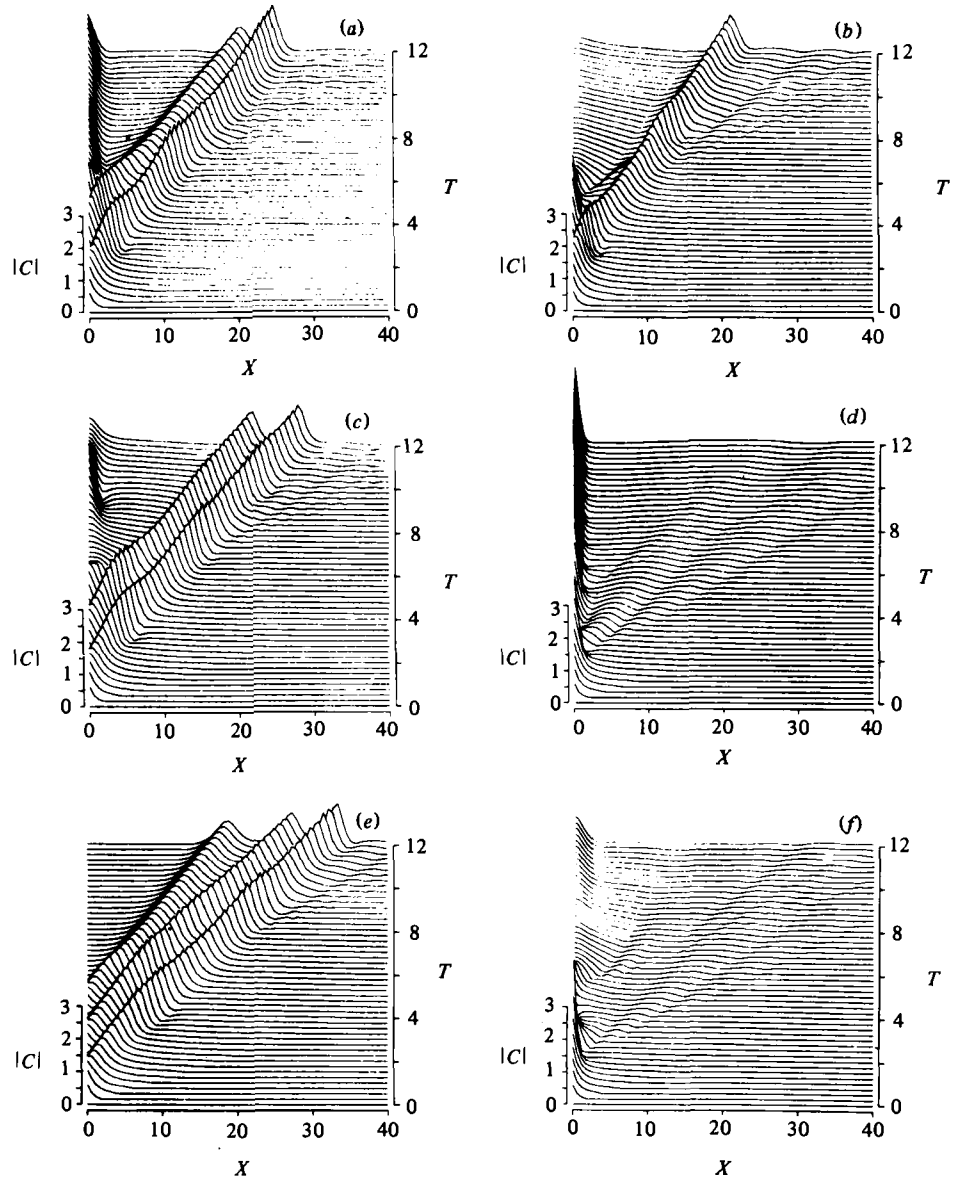

FIGURE 7. Space–time evolutions of $|C(X, T)|$; $T_0 = 5$, $K > 0$.
(*a*) $\lambda = \frac{1}{2}$; (*b*) 0; (*c*) 1; (*d*) -1; (*e*) 2; (*f*) -2.

we found that the threshold rose above the linear cut-off frequency with increasing duration T_0.

In nonlinear optical guides, (2.31*a*) with $\lambda = 0$ also holds if $\hat{T}$ is replaced by X and $\hat{X}$ by Y, where X and Y correspond respectively to the directions along and transverse to that of wave propagation. It is known (Karpman 1975) that, for $K > 0$, a sufficiently large initial pulse disintegrates into several peaks propagating away in the (X, Y)-plane; this is called *self-channelling*. It is also known that eigenmodes exist which represent waves trapped near $Y = 0$; this is called *self-focusing*. Our computations

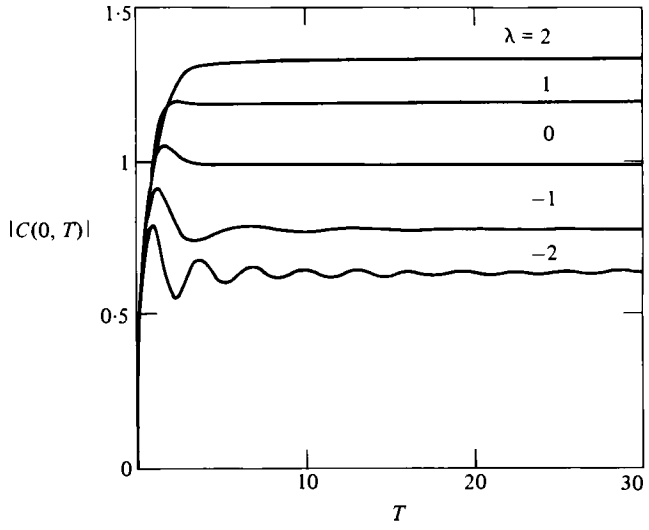

FIGURE 8. $|C(0, T)|$ for $T_0 \to \infty$, $K < 0$.

showed that, in acoustic wave-guides, there was peak emission above a cut-off frequency (self-channelling in the (T, X)-plane), and wave-trapping below a cut-off frequency (self-focusing). In some small neighbourhood of the threshold, both features could be present.

6. Nonlinear response to a sustained input ($T_0 \to \infty$)

When $\lambda \neq 0$, the linearized theory predicted a steady state of constant magnitude for any finite X if the uniform envelope of sinusoidal forcing at the piston persisted indefinitely. Recall from figure 1 and from the clause after (3.6) that, for $\lambda \neq 0$, the approach to the steady state was always accompanied by decaying oscillations, while for $\lambda = 0$ the linearized solution grew asymptotically as $T^{\frac{1}{2}}$. The important question here is whether a steady state can always be expected when nonlinearity is present.

6.1. *The case* $K < 0$

Equations (2.31*a–e*) were solved for a step-function forcing

$$f_n(T) = H(T) \quad \text{for} \quad -3 < \lambda < 4.$$

In all the cases, except near $\lambda = 3$, a steady state was quickly reached, as shown in figure 8 for $|C(0, T)|$. The asymptotic value for $T \gg 1$ (actually $T = 30$) of the pressure on the piston is displayed by crosses in figure 9 as a function of λ. For comparison the linear steady-state limits according to (3.7) are plotted as solid lines. Departure from the linear theory (cf. (3.7)) near $\lambda = 0$ is most remarkable. The differences between linear and nonlinear results are evident in the range $-3 < \lambda < 3$. Outside this range the difference diminished. In the nonlinear theory there was a critical λ, very near 3, beyond which the steady-state $C(0, T)$ dropped down toward the linear limit. When λ was but slightly greater than 3, $C(0, T)$ oscillated significantly with very slow decay, and the plotted points are obtained by averaging the converging envelopes at $T = 30$.

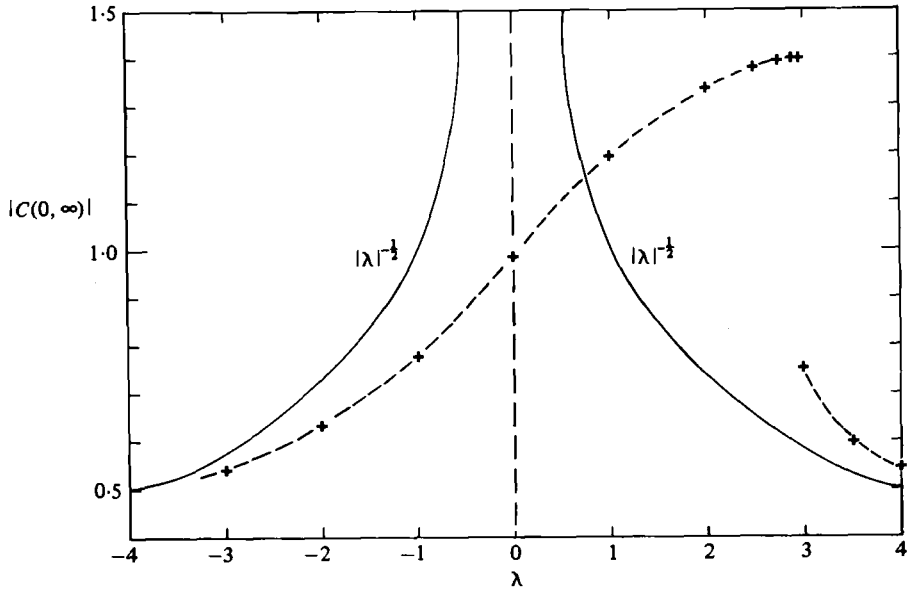

FIGURE 9. Steady-state limit of $C(0,T)$ as a function of λ for $T_0 \to \infty$, $K < 0$. +, nonlinear theory terminated at $T = 30$. The values taken are the mean of the converging envelopes of an oscillatory curve. Solid lines represent the linear theory according to (3.7).

The deviation from the average is largest ($\pm 0{\cdot}15$) at $\lambda = 3$, but diminishes to $\pm 0{\cdot}05$ at $\lambda = 3{\cdot}5$ and $\pm 0{\cdot}002$ at $\lambda = 4$. Why this special behaviour occurred near $\lambda = 3$ is not yet clear theoretically. It has not been possible for us to discern whether the upper branch curled back to the right to form a triple-value region of hysteresis for $\lambda > 3$. The spatial profiles for the different λs are qualitatively very similar, and only the case $\lambda = 0$ is presented in figure 10, showing energy-trapping near the piston.

Since the steady-state limit is seen numerically to exist, $i\partial C/\partial T$ may be dropped from (2.31), which can then be integrated to give

$$-i(C^*C_X - CC_X^*) = -2\mathscr{I}CC_X^* = 2|C|^2\frac{\partial\theta_C}{\partial X} \tag{6.1}$$

for all X, where θ_C is the phase of C. *If* θ_C is assumed as constant, it can be shown that

$$C_0 \equiv |C(0,\infty)| = [(\lambda + \tfrac{1}{2}(\lambda^2+4)^{\frac{1}{2}}]^{\frac{1}{2}}, \quad \theta_C = \pi \tag{6.2}$$

at the piston. For all other X the steady-state limit $C(X)$ is given by

$$\frac{(-\lambda)^{\frac{1}{2}} + (-\lambda + C^2)^{\frac{1}{2}}}{|C|} = \frac{(-\lambda)^{\frac{1}{2}} + (-\lambda + C_0^2)^{\frac{1}{2}}}{C_0} e^{-(-\lambda X)^{\frac{1}{2}}} \quad (X > 0,\ \lambda > 0), \tag{6.3}$$

$$C = \lambda^{\frac{1}{2}} \sec\{\arccos \lambda^{\frac{1}{2}}/C_0 - \lambda^{\frac{1}{2}}X\} \quad (X > 0,\ \lambda > 0). \tag{6.4}$$

These results can be inferred from Barnard *et al.* (1977). We found (6.2) and (6.3) to be in close agreement with our numerical results for $\lambda < 0$. However, for $\lambda > 0$ disagreement was significant. Upon examining (6.1) at $X = 0$, which is just the rate of work $\partial E/\partial T$ done by the piston to the fluid (see (4.3)), it was found from the numerical solution that $E(T)$ approached a constant for $\lambda < 0$, hence $\partial\theta_C/\partial X \simeq 0$. But $E(T)$ increased almost linearly with T for $\lambda \geqslant 0$ when $T \to \infty$; hence $\partial\theta_C/\partial X \simeq$ const

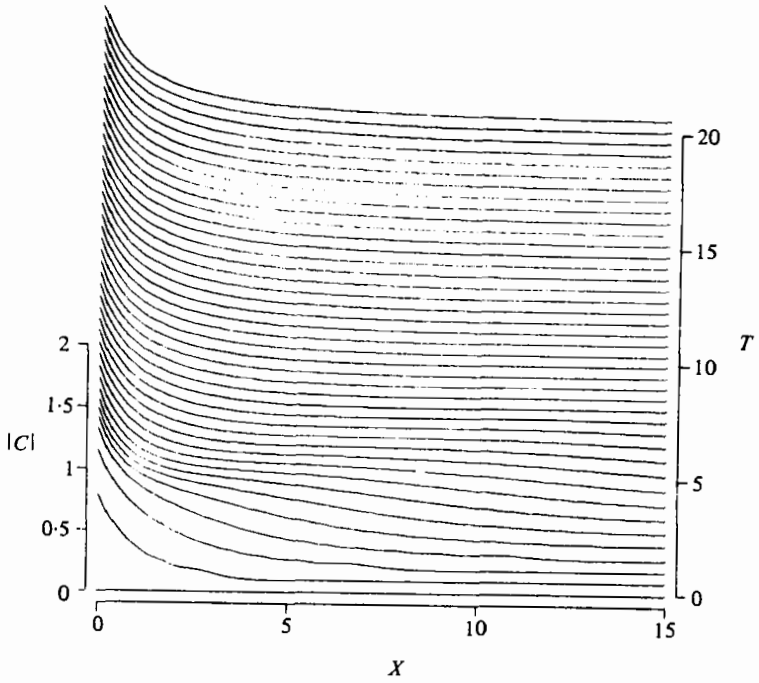

FIGURE 10. Space–time evolution of $|C(X, T)|$; $T_0 \to \infty$, $K < 0$, $\lambda = 0$.

at $X = 0$. This qualitative dependence on the sign of λ was consistent with the linearized approximation by (3.9).

6.2. *The case* $K > 0$

Figure 11 shows $|C(0, T)|$ for $\lambda = 0$. Now it is striking that a steady state was never reached even up to $T = 125$. Although the boundary condition implied no time scale, two modulation periods are apparent from the result, indicating that the trapped disturbance near $X = 0$ underwent multiperiod recurrence. The space–time plot figure 12 shows that there was an outgoing peak trailed by a train of smaller humps which emerged continuously from the piston. (Here, as in all the earlier space–time profiles, the very-small-amplitude waves leading the main disturbances were due to numerical noise probably caused by the abrupt jump in the boundary condition.) The humps following the peak in this case were of much larger amplitudes and remained when we varied the step size of our numerical scheme. A comparison of figures 11 and 12 revealed a one-to-one correspondence between the generation of such humps and the envelope oscillation at $X = 0$. The leading peak, like those in figures 5 and 7, advanced at a constant velocity ($\simeq 2$). The height of the peak oscillated with decaying amplitude, reaching an asymptotic value of about 1 with a profile approaching that of a soliton (4.4) as T increased. Similar computations for the pressure at the piston for $\lambda = -1$ and 1 again showed that a steady state was not reached. The evolution profiles $C(X, T)$ were very similar to the case of $\lambda = 0$, and are not presented here.

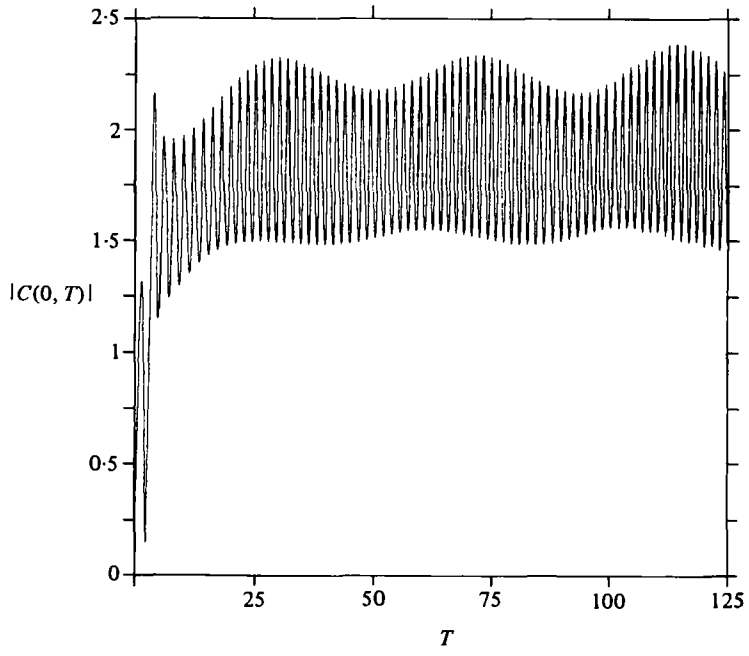

FIGURE 11. $|C(0, T)|$ for $T_0 \to \infty$, $K > 0$, $\lambda = 0$.

7. Concluding remarks

An inviscid numerical theory based on an asymptotic approximation has been presented for the transient nonlinear response in an acoustic duct. For a piston oscillating with a rectangular pulse envelope it is found that, when $K > 0$, the response changes drastically when the piston frequency changes from above to below the cut-off frequency. In contrast, there is no such distinction in the linearized limit. For a piston oscillating with a constant envelope, a steady state is reached only if $K < 0$. Strictly speaking, different initial conditions or pulse shapes may lead to different responses. On the basis of our numerical experiments we can only conclude that a steady state cannot always be expected in the inviscid case if $K > 0$.

Equation (2.31*a*) can be shown to govern the near-cut-off behaviour for a variety of waveguides when dissipation is ignored. The case studied by Barnard *et al.* (1977) for surface water waves in a channel is one such example. This is because (2.17) and (2.18) are also valid, and the time derivative in the free-surface condition

$$\phi_{tt} - g\phi_z = \text{nonlinear terms}$$

adds, at $O(\epsilon^{\frac{3}{2}})$, the term $i\partial C/\partial T$ to all the other secular terms shown in (1.1). Another simple example is a taut string supported laterally by a cubic-elastic foundation (Aranha 1978).

The effect of dissipation in the boundary layer next to the duct wall can be examined as in Barnard *et al.* for surface water waves. In particular the spatial attenuation rate can be estimated from the following linear boundary-value problem for the inviscid region outside the boundary layer:

$$\frac{\partial^2\phi}{\partial y^2} + \frac{\partial^2\phi}{\partial z^2} + \frac{\omega_n^2}{U_0^2}\phi = -\left(\frac{\partial^2}{\partial x^2} + \frac{\Omega^2 - \omega_n^2}{U_0^2}\right)\phi \quad \text{for } y, z \text{ in } S, \tag{7.1}$$

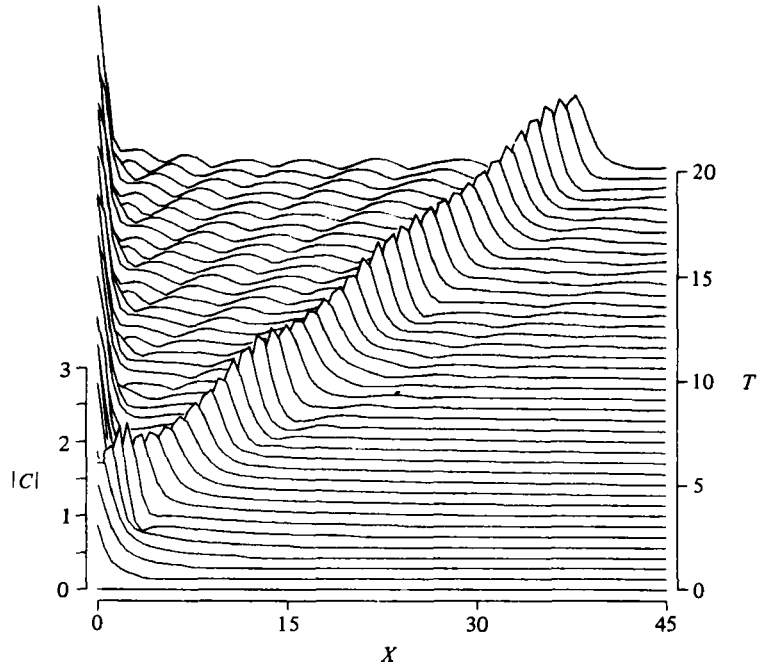

FIGURE 12. Space–time evolution of $|C(X, T)|$; $T_0 \to \infty$, $K > 0$, $\lambda = 0$.

$$\frac{\partial \phi}{\partial n} = \Delta \left(\frac{\partial^2 \phi}{\partial x^2} + \frac{\partial^2 \phi}{\partial s^2} \right) \quad \text{on } \partial S, \tag{7.2}$$

where n and s are locally orthogonal co-ordinates normal and tangential to the duct wall in the cross-sectional plane, and

$$\Delta = \left(\frac{\nu}{i\omega} \right)^{\frac{1}{2}} \frac{1}{a}, \tag{7.3}$$

is essentially the square-root of the reciprocal of the Reynolds number $R = \omega a^2/\nu$. Equation (7.1) is just the Helmholtz equation, while (7.2) represents the normal flux induced at the outer edge of the wall boundary layer by the viscous effect within. To help estimate the importance of viscosity, note that $\omega a/U_0 = O(1)$ for the lowest cut-off mode. Taking $a = 30$ cm, then $R^{-1} = |\Delta^2| = 10^{-4}$ for water and 4×10^{-4} for air. Hence $\Delta = O(\epsilon)$ if $\epsilon = O(0{\cdot}01)$; this will be assumed from here on. Letting

$$\phi = e^{ikx} \psi(y, z), \tag{7.4}$$

it is easy to find, by expanding ψ and k in half-powers of ϵ (see e.g. Mei & Liu 1973), that

$$k^2 = \frac{\lambda \epsilon}{U_0^2} - \Delta \oint_{\partial S} \left(\frac{\partial \psi_0}{\partial s} \right)^2 ds \Big/ \iint_S \psi_0^2 \, dA, \tag{7.5}$$

where ψ_0 is the inviscid cross-duct mode corresponding to ω_n. As was first noted by Barnard *et al.* the attenuation rate is proportional to $\epsilon^{\frac{1}{2}}/\Delta^{\frac{1}{2}} \sim R^{-\frac{1}{4}}$, in contrast to $R^{-\frac{1}{2}}$ when Ω is away from cut-off. Thus viscous influence is comparable to the effects of nonlinearity and frequency detuning, and important modification of the inviscid result can be expected, especially with regard to the variation along the duct.

However, for axially symmetrical modes $\partial\psi_0/\partial s \equiv 0$.† It can then be found by similar argument that

$$k = \epsilon^{\frac{1}{2}} \frac{\lambda^{\frac{1}{2}}}{C_0}\left[1 - \Delta \oint_{\partial S} \psi_0^2 \, ds \Big/ \iint_S \psi_0^2 \, dA\right]. \tag{7.6}$$

From the second term above, the length scale of viscous attenuation is $\Delta^{-1} \sim R^{\frac{1}{2}}$ times longer than the scale $O(\epsilon^{-\frac{1}{2}})$ associated with detuning and nonlinear evolution. Therefore the results presented in this paper are quantitatively relevant for axially symmetrical modes in a closed acoustic duct.

J.A.A. was supported by a fellowship from the Brasilian Instituto de Pesquisas Technológicas during most of his graduate study at M.I.T., where this work was initiated. All three authors have been supported at various stages of this work by the U.S. National Science Foundation (Earthquake Engineering and Engineering Mechanics Programs) and the U.S. Office of Naval Research (Fluid Dynamics Program). D.K.P.Y. also thanks Science Applications Inc. for computing time used for the revision of this paper.

REFERENCES

ARANHA, J. J. 1978 Nonlinear Resonance in Wave Guides. Part I of Ph.D. thesis, Department of Civil Engineering, Massachusetts Institute of Technology.

BARNARD, B. J. S., MAHONY, J. J. & PRITCHARD, W. G. 1977 The excitation of surface waves near a cut-off frequency. *Phil. Trans. R. Soc. Lond.* A **286**, 87–123.

KARPMAN, V. I. 1975 *Nonlinear Waves in Dispersive Media.* Pergamon.

KELLER, J. B. & MILLMAN, M. H. 1971 Finite amplitude sound wave propagation in a wave guide. *J. Acoust. Soc. Am.* **49**, 329–342.

MAHONY, J. J. 1971 Excitation of surface waves near to cut-off frequency. *University of Essex Fluid Mech. Res. Inst. Rep.* no. 7.

MEI, C. C. & LIU, P. L. F. 1973 The damping of surface gravity waves in a bounded liquid. *J. Fluid Mech.* **59**, 239–256.

MORSE, P. M. & INGARD, K. U. 1968 *Theoretical Acoustics.* McGraw-Hill.

OCKENDON, J. R. & OCKENDON, H. 1973 Resonant surface waves. *J. Fluid Mech.* **59**, 397–413.

URSELL, F. 1952 Edge waves on a sloping beach. *Proc. R. Soc. Lond.* A **214**, 79–97.

† This is not the case of cross-waves studied by Barnard *et al.*